

Hemoprotein Models Based on a Covalent Helix–Heme–Helix Sandwich: 2. Structural Characterization of Co^{III} Mimoschrome I Δ and Λ Isomers

Gabriella D'Auria, Ornella Maglio, Flavia Nastri, Angela Lombardi, Marco Mazzeo, Giancarlo Morelli, Livio Paolillo, Carlo Pedone, and Vincenzo Pavone*

Abstract: Fe^{III} mimoschrome I is the prototype of a new class of hemoprotein models characterized by a covalent helix–heme–helix sandwich. It contains deuterohemin bound through two propionyl groups to two identical *N*- and *C*-terminal protected α -helical nonapeptides, each of which bears a His residue (a potential axial ligand of the iron ion) in the central position. In order to understand better the three-dimensional structure of Fe^{III} mimoschrome I and its correlation with spectral properties, we have characterized the fully

diamagnetic parent compound Co^{III} mimoschrome I by UV/visible, CD, and NMR spectroscopy, coupled with conformational energy calculations. Co^{III} mimoschrome I is a highly water-soluble compound present in solution as two isomers, which slowly interconvert only at

very low pH values. These isomers were isolated and separately characterized. Their UV/visible spectral properties are very similar, while their CD spectral properties differ markedly in both the far UV and Soret regions. The isomers were identified by ¹H NMR spectroscopy as diastereomers of the Δ and Λ type. This is the first example of an accurate three-dimensional structure determination in solution of a hemoprotein mimetic that allows a straightforward correlation between structure and spectral properties.

Keywords

cobalt · helical structures · heme proteins · NMR spectroscopy · porphyrinoids

Introduction

We have recently undertaken the design, synthesis, and structural characterization of a novel class of hemoprotein models.^[1] The prototype Fe^{III} mimoschrome I, namely Fe^{III} 3,7,12,17-tetramethylporphyrin-2,18-di-N₈- ϵ -(Ac–Leu¹–Ala²–Gln³–Leu⁴–His⁵–Ala⁶–Asn⁷–Lys⁸–Leu⁹–NH₂)propionamide, is a peptide–heme adduct containing a covalent helix–heme–helix sandwich. It consists of deuterohemin bound through propionyl groups to two identical *N*- and *C*-terminal protected α -helical nonapeptides. Each peptide moiety bears a His residue in the central position, which may act as an axial ligand to the central iron ion.

This work was aimed at a better understanding of the structure–function relationship in hemoproteins, in which the heme group reactivity is strongly affected by the polypeptide matrix. Studies on the effects produced by axial ligation and by the local heme environments on electronic and catalytic properties have

elucidated the role of the protein chain in defining a large variety of functions observed within the hemoprotein family.^[2, 3] These results have not only stimulated studies on natural hemoproteins and their mutants, but have also drawn an increasing degree of attention to the use of model compounds, such as simple metalloporphyrin complexes and their derivatives, with the expectation that relatively simple model systems could emulate in vitro many of the reactions observed in vivo (selective oxidation of hydrocarbons, electron transfer, uptake and storage of oxygen, etc.).^[4] Within the wide variety of model systems thus far used,^[5–7] a new class of models based on synthetic polypeptides with well-defined tertiary structures appears to be capable of partially reproducing the behavior and properties of hemoproteins. Several successful examples of de novo design of small proteins have recently been reported.^[8–10]

Fe^{III} mimoschrome I was designed and synthesized to meet the following requirements: a) to stabilize the peptide α -helical conformation with its axis almost parallel to the porphyrin plane; b) to bring histidine residues into a suitable position to coordinate axially the metal atom inserted in the porphyrin ring; c) to improve water solubility by introducing hydrophilic sidechains on the molecular surface. Mimoschrome I was also characterized by several methods: UV/visible spectroscopy and circular dichroism confirmed that it takes the designed structure in water/2,2,2-trifluoroethanol (TFE) solution.^[1a] Unexpectedly, Fe^{III} mimoschrome I appeared to be of limited solubility in water

[*] Prof. V. Pavone, Dr. G. D'Auria, Dr. O. Maglio, Dr. F. Nastri, Dr. A. Lombardi, Dr. M. Mazzeo, Prof. G. Morelli, Prof. L. Paolillo, Prof. C. Pedone
Centro Interdipartimentale di Ricerca sui Peptidi Bioattivi CEINGE - Biotecnologie Avanzate e Centro di studio di Biocristallografia CNR
Via Mezzocannone 4, I-80134 Napoli (Italy)
Phone: Int. code + (81) 551-6526
Fax: Int. code + (81) 552-7771
e-mail: pavone@chemna.dichi.unina.it

and alcohols, and therefore only a partial structural characterization was carried out. In order better to understand the three-dimensional structure of Fe^{III} mimochrome I and its correlation with UV/visible and CD spectral properties we have undertaken the characterization of the fully diamagnetic parent compound Co^{III} mimochrome I, whose structure is depicted in Figure 1.

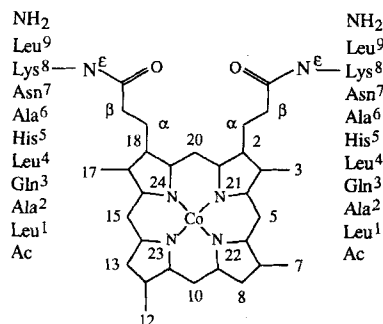


Figure 1. Schematic structure of Co^{III} mimochrome I with atom numbering.

Co^{III} mimochrome I was synthesized and obtained as two isomers that were separately characterized. They are highly soluble in water, and have identical molecular ion peaks by mass spectrometry and very similar UV/visible spectra. They show different CD spectra in both the far UV and the Soret regions. Complete identification of these isomers as the Δ and Λ diastereomers was ultimately achieved by ¹H NMR spectroscopy.

Abstract in Italian: La molecola Fe^{III} mimochrome I rappresenta il prototipo di una nuova classe di modelli di emoproteine, caratterizzata da un "sandwich" covalente elica-eme-elica. Essa è costituita dalla deuterioemina, i cui gruppi propionici sono legati a due identici nonapeptidi, protetti alle estremità N- e C-terminali, tali da stabilizzare strutture elicoidali. Ogni catena peptidica presenta in posizione centrale un residuo di His quale legante assiale per il metallo inserito nel nucleo porfirinico. Allo scopo di meglio chiarire la struttura tridimensionale di Fe^{III} mimochrome I e la correlazione esistente tra struttura e proprietà spettroscopiche, è stata intrapresa la caratterizzazione dell'analogo diamagnetico Co^{III} mimochrome I.

In questo lavoro sono descritte le proprietà UV/visibili e CD del composto Co^{III} mimochrome I, ed una dettagliata caratterizzazione strutturale in soluzione, mediante spettroscopia NMR unita a calcoli di energia conformazionale. Co^{III} mimochrome I presenta una elevata solubilità in acqua ed è presente in soluzione sotto forma di due isomeri, lentamente interconvertibili a bassi valori di pH. Tali isomeri sono stati isolati e caratterizzati separatamente. Essi hanno mostrato uguali spettri UV/visibili, mentre i loro spettri CD sono marcatamente differenti sia nella regione UV che nella regione di Soret. La spettroscopia ¹H NMR ha permesso di caratterizzare completamente entrambi gli isomeri e di identificarli quali diastereomeri di tipo Δ e Λ . I risultati riportati nel presente lavoro rappresentano il primo esempio di una accurata caratterizzazione strutturale in soluzione di un mimetico di emoproteine; essi permettono una chiara correlazione tra struttura tridimensionale e proprietà spettrali.

Results

Synthesis and HPLC studies: Cobalt(III) was inserted into mimochrome I from Co^{II} acetate according to the literature method.^[11] Figure 2 shows the HPLC chromatogram of the reaction mixture used in the preparation of Co^{III} mimochrome I. Two equally abundant peaks, Δ and Λ , were detected. No substantial changes in the 1:1 ratio between the peak areas of the Δ and Λ species resulted from either extension of the reaction time or use of conditions that favored Co^{II} \rightarrow Co^{III} air oxidation. The two species were then separated by preparative HPLC and separately analyzed. The FAB mass spectra revealed a molecular weight of 2625 for both the Δ and Λ species. It corresponds to the expected value for Co^{III} mimochrome I. In order to discover whether Δ and Λ are very slowly

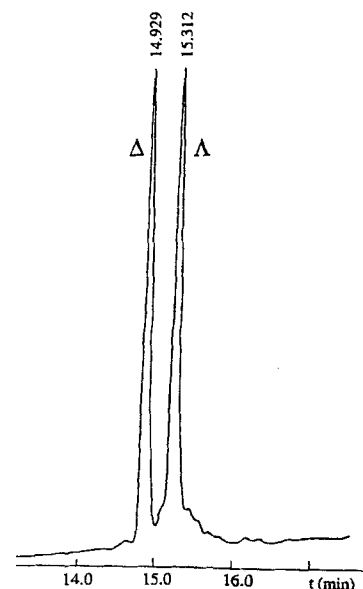


Figure 2. HPLC chromatogram of the reaction mixture during the synthesis of Co^{III} mimochrome I.

interconverting isomers, HPLC studies were performed by dissolving both the Δ and Λ species separately in different media. Δ and Λ species were found to be stable in TFE solution and after 48 hours neither Λ nor Δ formation, respectively, was detected. In contrast, the addition of acetic acid to an aqueous solution of either pure Λ or Δ species resulted in progressive formation of either Δ or Λ species, respectively. The $\Delta \leftrightarrow \Lambda$ acid-catalyzed interconversion was slow; equilibrium was reached within four days.

UV/Visible properties: In order to better characterize both Δ and Λ isomers, we evaluated their spectroscopic properties in the UV/visible region. When a Co^{II} salt is used, the insertion of cobalt into the porphyrin ring could lead to several species which can be identified by their UV/visible spectral differences.^[12] Table 1 summarizes the spectral data either in aqueous phosphate or in TFE/aqueous phosphate solutions (1:1 v/v) for both Δ and Λ isomers. The λ_{max} at 414 nm of the Soret band and the λ_{max} at 524 and 556 nm and the relative intensities of the β and α bands are characteristic of an octahedral Co^{III} complex for

Table 1. UV/Visible spectral data for Δ and Λ Co^{III} mimochrome I isomers in TFE/aqueous phosphate (1/1; v/v) at pH 7.0.

Species	$\epsilon_{(\text{Soret})}$ (M ⁻¹ cm ⁻¹)	$\epsilon_{(\beta)}$ (M ⁻¹ cm ⁻¹)	$\epsilon_{(\alpha)}$ (M ⁻¹ cm ⁻¹)	UV/Vis λ_{max} (nm)		
				Soret	β	α
Δ	11 2385	7299	5422	414	524	556
Λ	93911	6387	4816	414	525	557

both the Δ and Λ isomers.^[13] No spectral changes were observed at very low pH (TFE/phosphoric acid 1.43 M, 1:1 ratio; data not shown). Figure 3 shows the similarity of the UV/visible spectra of the two isomers. The only difference is the extinction coefficient at the Soret maximum wavelength as determined by Lambert and Beer's law, which is slightly smaller for the Λ isomer.

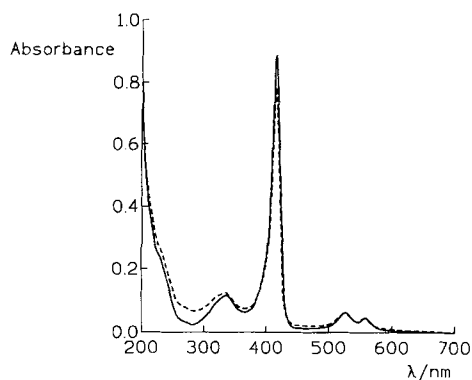


Figure 3. UV/Vis spectra of Co^{III} mimochrome I Δ isomer (—) and Λ isomer (---).

CD spectra: In order to investigate the structural differences between the two isomers, circular dichroism measurements were recorded in both the far UV and the Soret region. The CD spectra of the Δ and Λ isomers at different TFE concentrations are reproduced in Figure 4. Plots of $[\theta]_{222}$ and $[\theta]_{419}$ versus TFE

concentration are also reported in Figure 4e and 4f for the Δ and Λ isomers, respectively. Table 2 contains the typical CD parameters for both species. The spectrum of the Δ isomer in aqueous phosphate exhibits a maximum at about 188 nm, together with a double minimum at 222 and 202 nm (see Figure 4a). As the concentration of TFE increases, the minimum absorption peak (π - π^* transition) shifts from 202.6 to 204.2 nm, and the ellipticity at 222 nm (n - π^* transition) decreases. Moreover, the crossover λ_0 shifts to longer wavelengths, and $[\theta]_{\text{ratio}}$ ($[\theta]_{222}/[\theta]_{204}$) increases from 0.40 to 0.51. As widely reported in the literature,^[14] all these spectroscopic features are characteristic of an α -helical arrangement. However, a more pronounced minimum at lower wavelength ($[\theta]_{\text{ratio}} < 1$) has been proposed^[15] as a typical feature of a 3_{10} -helical distortion. Furthermore, an isodichroic point at 199.0 nm was observed upon TFE addition. This suggests that the spectral changes induced by TFE reflect a two-state transition between the random coil and the helical conformation.^[16]

Figure 4b represents the TFE CD titration performed on the Λ isomer. The CD spectrum of the Λ isomer in aqueous phosphate reveals the presence of a crossover λ_0 around 190 nm instead of a maximum of ellipticity. This is indicative of a random coil conformation for the peptide chains in the Λ isomer.^[16] Furthermore, the $[\theta]_{\text{ratio}}$ of about 0.2 and the position of the π - π^* transition minimum around 200 nm strongly support a disordered conformation for the Λ isomer in aqueous phosphate. When the TFE concentration is increased, a coil \rightarrow helix

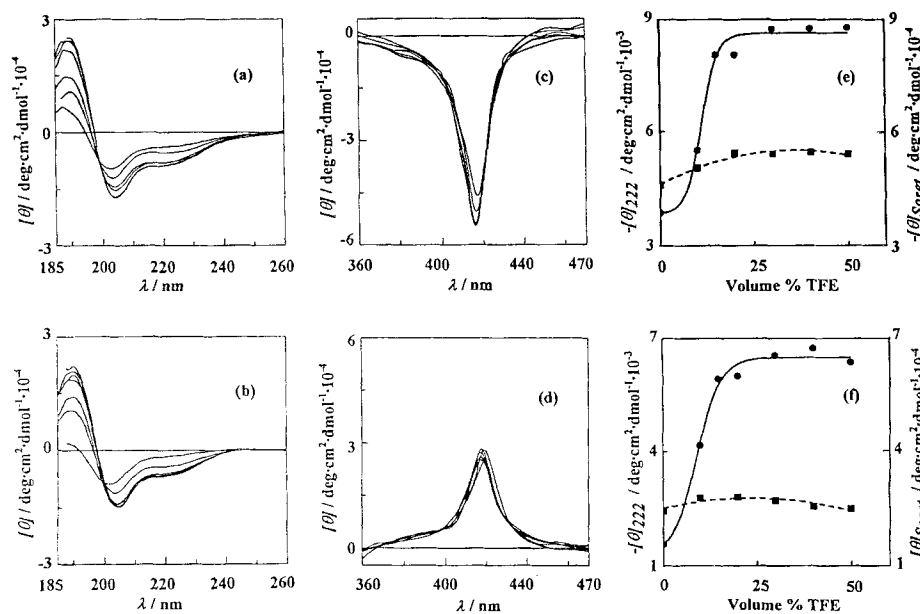


Figure 4. (a) and (b): Far UV CD spectra at various TFE concentrations of Co^{III} mimochrome I Δ and Λ isomers, respectively; (c) and (d): CD spectra in the Soret region at various TFE concentrations of Co^{III} mimochrome I Δ and Λ isomers, respectively; (e) and (f): plot of $[\theta]_{222}$ (●) and $[\theta]_{\text{Soret}}$ (■) vs. TFE concentration (v/v %) for Co^{III} mimochrome I Δ and Λ isomers, respectively.

Table 2. CD Parameters for Δ and Λ Co^{III} mimochrome I isomers in TFE/phosphate buffer [a].

Species	% TFE	$[\theta]_{\text{min}} \times 10^{-3}$ (λ_{min}) [b]	$[\theta]_{222} \times 10^{-3}$	$[\theta]_{\text{ratio}}$ [b]	λ_0	$[\theta]_{199} \times 10^{-3}$	$[\theta]_{\text{Soret}} \times 10^{-3}$ (λ_{Soret}) [c]
Δ	0	-9.7 (202.6)	-3.9	0.40	194.5	6.6	-45.9 (417.2)
Δ	30	-17.1 (204.0)	-8.7	0.51	197.3	25.1	-57.0 (416.6)
Λ	0	-8.9 (201.6)	-1.6	0.17	191.7	-	24.5 (419.2)
Λ	30	-14.7 (204.4)	-6.5	0.44	197.7	22.2	27.1 (417.4)

[a] Parameters are derived from the experimental CD spectra recorded under the conditions indicated in the experimental section; pH = 7. [b] In the UV region $[\theta]$ is expressed as mean residue ellipticity ($^{\circ}$ cm² dmol⁻¹), calculated by dividing the total molar ellipticity by the number of amino acids in the molecule; $[\theta]_{\text{ratio}}$ represents the ratio of the ellipticity at 222 nm to that at the shorter wavelength minimum. λ reported in nm. [c] $[\theta]$ in the Soret region is reported as total molar ellipticity. λ reported in nm.

transition occurs. The $[\theta]_{\text{ratio}}$ significantly increases from 0.17 to 0.45 on addition of 10% TFE. This suggests a strong helix-inducing effect of the solvent on the Λ isomer. A more pronounced minimum at lower wavelength ($[\theta]_{\text{ratio}} < 1$) has also been observed for the Λ isomer, and thus a 3_{10} -helical distortion may be present. The lack of an isodichroic point during TFE addition could indicate a noncooperative or a multiple-state random coil \leftrightarrow helix transition.^[16]

In the Soret region, the Δ isomer is characterized by a negative Cotton effect at 417.2 nm, with a molar ellipticity of $-45.9 \times 10^3 \text{ }^\circ \text{cm}^2 \text{dmol}^{-1}$ in the absence of TFE. Increasing the TFE concentration causes the molar ellipticity to decrease to $-57.0 \times 10^3 \text{ }^\circ \text{cm}^2 \text{dmol}^{-1}$ at 30% TFE concentration; at higher TFE concentration no further decrease of the molar ellipticity is observed. In contrast, the Λ isomer shows a positive Cotton effect at 419.2 nm, with a molar ellipticity of $24.5 \times 10^3 \text{ }^\circ \text{cm}^2 \text{dmol}^{-1}$ in the absence of TFE. An increase in the TFE concentration leads to a slight increase in the molar ellipticity to $27.1 \times 10^3 \text{ }^\circ \text{cm}^2 \text{dmol}^{-1}$ at 30% TFE concentration, where a small shift to 417 nm of the maximum wavelength is also observed. At higher TFE concentrations a small decrease of the molar ellipticity is observed.

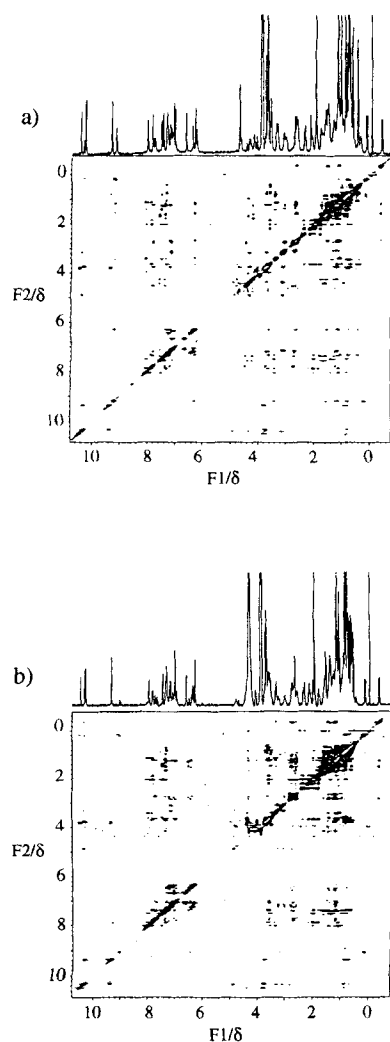


Figure 5. Monodimensional ¹H NMR spectra (upper part) and 2D NOESY spectrum (lower part) of Co^{III} mimochrome I Δ isomer (a) and Λ isomer (b).

¹H NMR analysis of the Δ isomer: The ¹H spectrum of the Co^{III} mimochrome I Δ isomer is shown along the top of Figure 5a. There is a single set of resonances for the deuteroporphyrin protons, and two sets of resonances for the peptidic part, with severe overlap for some of the homologous residues belonging to the two different peptide chains. His⁵, Ala⁶, and Asn⁷ exhibit two clearly distinct groups of resonances. The intensities of the deuteroporphyrin proton resonances as compared with those of the peptide chains are in the expected 1:2 ratio. Resonance assignments were accomplished by 2D experiments (TOCSY,^[17] NOESY,^[18] ROESY,^[19] and DQF-COSY^[20]) by means of the sequential technique for both deuteroporphyrin^[21] and peptide protons.^[22] Histidine sidechain protons were unequivocally assigned. The δ -CH resonances were easily identified on the basis of medium range NOE with the His⁵ $\beta\beta'$ -CH₂ protons. In the TOCSY experiment the δ -CH signals at $\delta = -0.34$ and -0.38 are correlated to ϵ -CH imidazole protons at $\delta = 0.20$ and 0.16 , respectively. These last resonances are in strong dipolar contact with a resonance at $\delta = 9.18$, which was assigned to the imidazole δ -NH of the two histidines.

However, it was not possible specifically to attribute the resonances of the peptide chain linked to the propionyl groups in either positions 2 or 18 of the deuteroporphyrin ring. Coupling constant values were evaluated from 1D spectra or from DQF-COSY when resonances overlapped. Table 3 reports all the ¹H chemical shifts and ³J_{NH₂CH} coupling constant values. The lower part of Figure 5a reports the NOESY spectrum with a mixing time of 250 ms.

All deuteroporphyrin proton resonances were unambiguously assigned, with the exception of those of the indistinguishable propionic groups. The assignment was easily performed follow-

Table 3a. Co^{III} mimochrome I Δ isomer ¹H assignments and ³J_{NH₂CH} (Hz) [a].

	³ J _{NH₂CH}	H ^x	H ^y	H ^β	H ^γ	H ^δ	others
Leu ¹	3.2	7.49	3.42	1.40 0.80	1.24	0.86 0.76	
Ala ²	3.6	8.06	3.37	1.10			
Gln ³	[b]	7.88	3.63	2.01 1.83	2.40 2.18		7.11, 6.66 δ -CONH ₂
Leu ⁴	5.6	7.33	3.62	0.74 0.41	1.04	0.68 0.50	
His ⁵	7.2	6.28	2.65	1.55		-0.34 H ^δ -0.38 H ^δ	0.20 H ^ε 9.18 δ -NH 0.16 H ^ε
Ala ⁶	3.0 3.0	7.20 7.17	3.73	1.45 1.21			
Asn ⁷	6.4 6.4	7.81 7.77	4.49 4.48	2.71			7.23, 6.42 γ -CONH ₂
Lys ⁸	6.0	7.36	4.23	1.76 1.58	1.21	1.09 1.35	3.06 2.71 7.13 ϵ -NH
Leu ⁹	7.6	7.55	4.39	1.68	1.58	0.96 0.83	7.05, 6.33 α -CONH ₂

Table 3b. Deuteroporphyrin ¹H assignments.

2,18 α,α' -CH ₂	4.87, 4.34	7CH ₃	3.81	13H	9.36
2,18 β,β' -CH ₂	3.16	8H	9.35	15H	10.31
3CH ₃	3.75	10H	10.28	17CH ₃	3.71
5H	10.45	12CH ₃	3.74	20H	10.36

[a] Bold values correspond to differentiated resonances for homologous residues belonging to different peptide chains. [b] Not measurable because resonances overlap.

ing the NOE connectivities around the ring and starting from the 5H proton at $\delta = 10.45$; it is the only proton in dipolar contact with the two methyl groups (3-CH₃ and 7-CH₃). The undifferentiated propionic $\alpha, \alpha'-CH₂ protons resonate at $\delta = 4.87$ and 4.34, while the four β -CH₂ protons are centered at $\delta = 3.16$.$

Chemical shifts of the peptide residues show a significant upfield shift when compared with typical random coil values.^[23] α -CH and amidic NH proton chemical shift changes are reported in bar charts in Figure 6a. Since this effect is shown by amidic NH and α -CH as well as by sidechain protons, and particularly in His⁵, it is reasonable to assume that these deviations are due to both the deuteroporphyrin ring current effect^[24] and to the peptide secondary structures.^[23, 25–26]

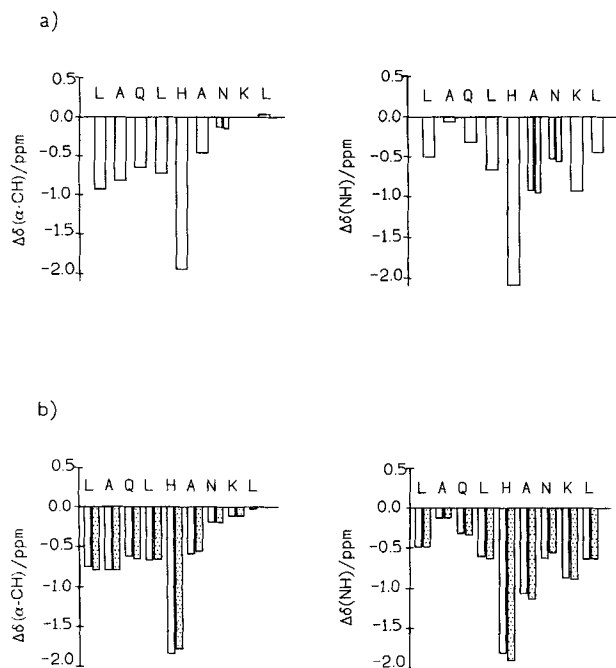


Figure 6. Chemical shift index $\Delta\delta(\alpha\text{-CH})$ and $\Delta\delta(\text{NH})$ for Co^{III} mimochrome I: a) Δ isomer. α -CH Asn⁷ and NH Ala⁶ and Asn⁷ show distinct resonances for the two peptide chains. b) Λ isomer. All protons show distinct resonances for the two peptide chains.

Indeed, the pattern of the NOE connectivities strongly supports the presence of a quite regular structure of the peptide chains. A total of 292 short-range and 48 long-range NOE connectivities were measured. The relative intensities of the structurally considerable NOE crosspeaks are shown in Figure 7. A continuous stretch of $d_{\text{Ni}, \text{Ni}+1}$ NOEs stronger than $d_{\alpha_i, \text{Ni}+1}$ connectivities were monitored. Furthermore, several long-range contacts were unambiguously observed throughout the peptide sequence such as relatively strong d_{α_i, β_i+3} , $d_{\alpha_i, \text{Ni}+2}$, $d_{\alpha_i, \text{Ni}+3}$ and weaker $d_{\text{Ni}, \text{Ni}+2}$ NOEs. These data point to a right-handed helical arrangement of both peptide chains. The $^3J_{\text{NH}\alpha\text{CH}}$ coupling constant values (see Table 3) are also in agreement with this helical structure. J values slightly higher than those expected for a helix were observed for His⁵, Asn⁷, Lys⁸, and Leu⁹. This may correspond to a higher flexibility or helix distortion at the C-terminal end of the peptide chain.

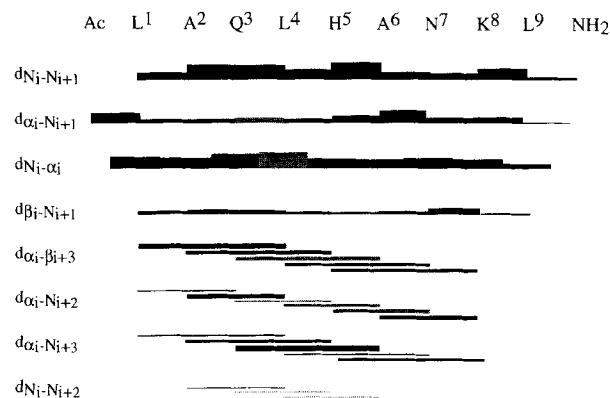


Figure 7. NOE connectivities observed for Co^{III} mimochrome I Δ isomer. Solid bars indicate unambiguous NOEs. Bar thickness is proportionally related to the NOE intensity.

From a structural point of view, the determination of the His sidechain orientation with respect to the peptide backbone is of interest. Several NOE contacts of the histidine protons with Leu¹, Ala², and Leu⁴ protons were observed. Some of these contacts are unambiguous since they are caused by the ϵ -CH and δ -CH protons, which give distinct resonances for each histidine residue. Unexchangeable δ -NH are also clearly visible, indicating that these protons are buried in the interior of the molecule and/or hydrogen-bonded. This further supports the proposition that the cobalt(III) axial ligation occurs through the unprotonated imidazole N ϵ atom of the histidines. The ϵ -CH and δ -CH imidazole protons experience an extremely large ring-current effect from the deuteroporphyrin and appear in the high-field region of the spectrum. An upfield displacement of 0.04 ppm for one of the two histidines suggests a slightly different position of the imidazole rings with respect to the deuteroporphyrin plane.

Furthermore, δ -CH and ϵ -CH protons in the histidines have different connectivities with the deuteroporphyrin protons. One histidine exhibits ϵ -CH \leftrightarrow 5H, ϵ -CH \leftrightarrow 3-CH₃, δ -CH \leftrightarrow 12-CH₃, δ -CH \leftrightarrow 13H, and δ -CH \leftrightarrow 15H dipolar contacts; the other histidine exhibits only ϵ -CH \leftrightarrow 15H and δ -CH \leftrightarrow 5H NOEs (see Figure 8a). Both imidazole rings presumably lie in planes orthogonal to the deuteroporphyrin ring, one imidazole plane intersecting the ring through the 15H and 5H protons, while the other imidazole plane intersects it through the 4 and 14 positions of the deuteroporphyrin. This is indicative of an approximately antiparallel alignment of the imidazole rings; their planes form an angle of about 150°. Figure 8a also describes the imidazole orientation to the deuteroporphyrin plane, taking into account all experimental observations. The angle μ is defined as the torsion angle C δ -N ϵ -Co-N21. One histidine has a μ angle of about 45° and the other of about 165°.

Several NOE contacts between peptide sidechains and deuteroporphyrin protons were measured in the NOESY spectra, with a mixing time of 250 ms. Dipolar contacts are shown in particular by leucines and lysine sidechains (Figure 9a). Because the resonance overlaps between homologous residues belonging to different peptide chains, it was not possible to interpret unequivocally these peptide–deuteroporphyrin NOE effects. Nevertheless, simple stereochemical consideration of the right-handed helical structure of the peptide allowed us to iden-

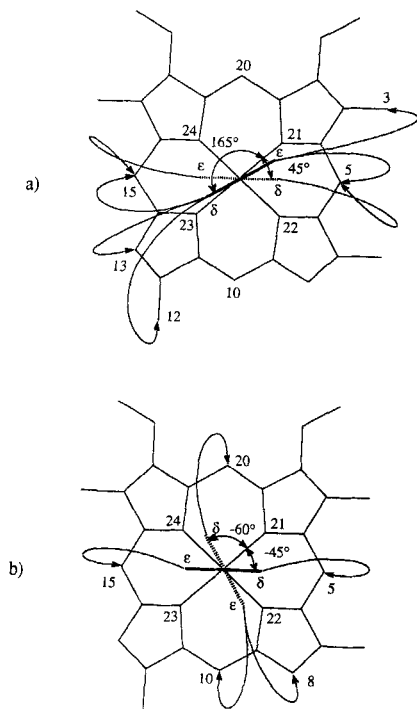


Figure 8. Schematic presentation of the NOE connectivities (arrows) between His⁵ ϵ -CH (ϵ) and δ -CH (δ) protons and the deuteroporphyrin protons for Co^{III} mimochrome I Δ isomer (a) and Λ isomer (b). When viewed along the $N_{\delta}-N_{\epsilon}$ direction, the imidazole rings appear as segments which are depicted as thick continuous or dashed lines (above or below the deuteroporphyrin ring, respectively). The μ angles ($C_{\delta}-N_{\epsilon}-Co-N_{21}$) are also shown.

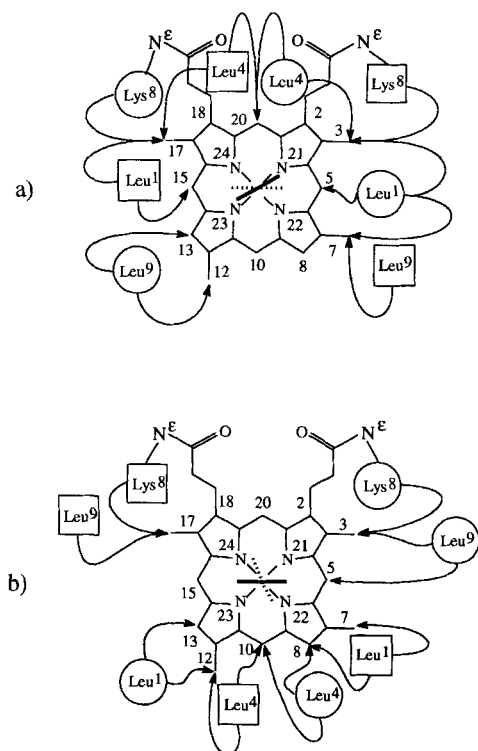


Figure 9. Schematic presentation of the NOE connectivities (arrows) between Leu¹, Leu⁴, Lys⁸, and Leu⁹ sidechain protons and the deuteroporphyrin protons for Co^{III} mimochrome I Δ isomer (a) and Λ isomer (b). Residues belonging to the same peptide moiety are either shown inside either a circle or a square. The coordinated imidazole rings are represented as thick continuous or dashed lines.

tify all the connectivities between Leu¹, Leu⁴, Lys⁸, Leu⁹ sidechains and the deuteroporphyrin protons with absolute confidence. Figure 9a depicts the final interpretation. The resonances at $\delta = 0.80$ and 0.78 attributed to δ -methyl groups of the two Leu¹ residues showed dipolar contacts with 5H, 7-CH₃, 3-CH₃ and 15H, 17-CH₃ protons of the deuteroporphyrin. Because of the large distance between these deuteroporphyrin protons (5H, 7-CH₃, 3-CH₃ from 15H, 17-CH₃), these NOE effects were interpreted in terms of different contacts of the two Leu¹ sidechains belonging to the two different peptide chains. Similarly, the Leu⁴ δ -protons appear to be connected with the 20H, 3-CH₃, and 17-CH₃ groups of the deuteroporphyrin ring. Accordingly, these connectivities are attributed to two different Leu⁴ of the two peptide chains. Leu⁹ δ -methyl protons appear to be connected to the 12-CH₃, 13H, and 7-CH₃ protons. Since these substituents are on opposite sides of the macrocycle, the Leu⁹-deuteroporphyrin interactions are again attributed to residues belonging to different peptide chains. Finally, spatial interactions between Lys⁸ sidechains and 17-CH₃ and 3-CH₃ were observed.

Figure 10a describes the approximate orientation of Leu¹, Leu⁴, His⁵, Lys⁸, and Leu⁹ sidechains facing the deuteroporphyrin plane. These sidechains belong to the two different pep-

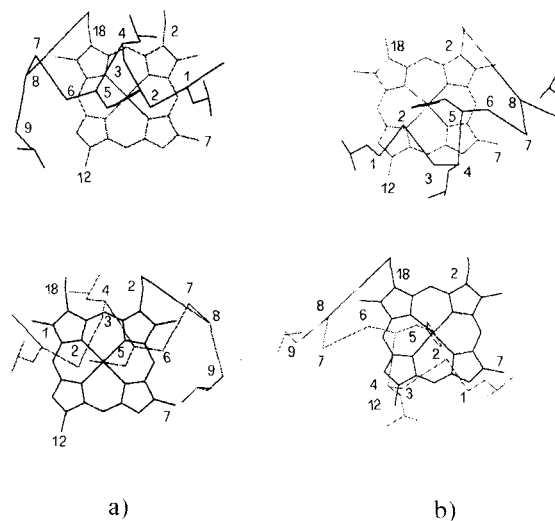


Figure 10. Approximate orientation of the two peptide chains with respect to the deuteroporphyrin plane for Co^{III} mimochrome I Δ isomer (a) and Λ isomer (b). Deuteroporphyrin or peptide moieties above the plane are pictured as continuous lines.

tide chains, named as A and B chains. Attribution of these residues to chain A or B, as shown in Figure 10a, was accomplished by taking into account all available CD and NMR information on the overall helical structure of the peptide chains. In an almost regular right-handed α -helical conformation, Leu¹, Leu⁴, His⁵, Lys⁸, and Leu⁹ would in fact be placed approximately as represented in Figure 10a. Furthermore, owing to the right-handedness of the α -helices, chain A must lie above the plane of the deuteroporphyrin as it appears in Figure 10a, and consequently chain B is located below this plane. The reverse situation could be obtained only by a reflection of the peptidic part in the deuteroporphyrin plane. This would give rise to the

impossible situation of helices of opposite handedness formed by D-amino acids. Finally, it was easy to identify chain A as the one bound to the propionyl group in position 18 and chain B as bound to the propionyl group in position 2 on the basis of the relative proximity of A-chain Lys⁸ and 18-propionyl group, and B-chain Lys⁸ and 2-propionyl group, respectively. At this point the stereochemistry of the Δ isomer was fully identified; its configuration is depicted in Figure 11.

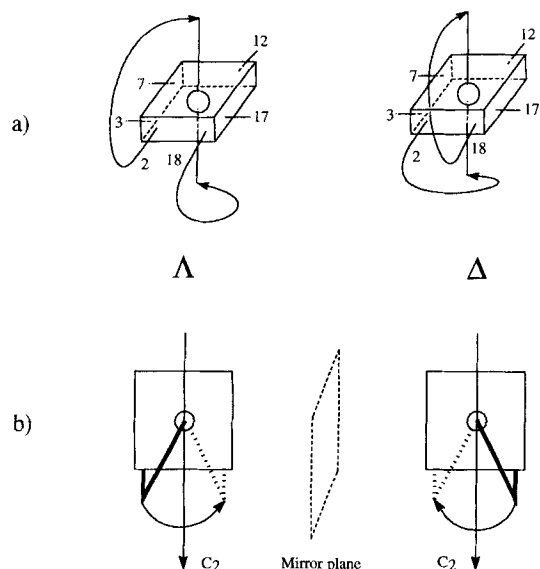


Figure 11. Schematic representations of the Δ and Λ isomer configuration.

¹H NMR analysis of the Λ isomer: The ¹H monodimensional spectrum of the Co^{III} mimochrome I Λ isomer is shown in the upper part of Figure 5b. There is a single set of resonances for the deuteroporphyrin protons, and two sets of resonances for the peptidic part. The chemical shift differences between homologous residues belonging to different peptide chains are more substantial for backbone protons (α -CH and amidic NH) and these differences increase in going from the N- and C-terminal residues (Leu¹ and Leu⁹) toward the central residue (His⁵). The resonance differences, ranging from 0.01 to 0.09 ppm, easily allowed the sequential assignment for each peptide chain by 2D experiments (TOCSY, DQF-COSY, ROESY, and NOESY). Histidine sidechain protons were unequivocally assigned. The δ -CH resonances were easily identified on the basis of medium-range NOE with the His⁵ $\beta\beta'$ -CH₂ protons. In the TOCSY experiment the δ -CH signals at $\delta = -0.32$ and -0.36 are correlated with ϵ -CH imidazole protons at $\delta = 0.18$ and 0.14 , respectively. These last resonances are in strong dipolar contact with the resonances at $\delta = 9.02$ and 9.06 respectively, which were assigned to the imidazole δ -NH of the two histidines.

However, it was not possible specifically to attribute the resonances of the peptide chain linked to the propionyl groups in either 2- or 18- positions of the deuteroporphyrin ring, because the undistinguishable propionic α,α' -CH₂ protons resonate at $\delta = 4.30$ and 4.90 , while the β,β' -CH₂ protons are centered at $\delta = 3.10$ and 3.30 . The other deuteroporphyrin proton resonances were identified by sequential assignment starting from the 5H proton at $\delta = 10.48$. Coupling constant values were eval-

Table 4a. Co^{III} mimochrome I Λ isomer ¹H assignments and ³J_{NH α CH} (Hz) [a].

	³ J _{NHαCH}	H ^N	H ^{α}	H ^{β}	H ^{γ}	H ^{δ}	others
Leu ¹	3	7.50	3.56	1.44, 0.96	1.36	0.90, 0.82	
			3.60	1.46, 1.04			
Ala ²	3	7.99	3.40	1.10			
Gln ³	5	7.87	3.66	2.01, 1.83	2.39, 2.18		7.06, 6.35 δ -CONH ₂
	5		7.85	3.63			
Leu ⁴	6	7.38	3.68	0.95, 0.70	1.15	0.74, 0.60	
	6	7.35	3.69	0.82, 0.65	1.22	0.81, 0.68	
His ⁵	7	6.55	2.75	1.46, 1.28		-0.32 H ^{β}	0.18 H ^{ϵ}
							9.02 δ -NH
	7	6.46	2.81	1.49, 1.21		-0.36 H ^{β}	0.14 H ^{ϵ}
							9.06 δ -NH
Ala ⁶	3	7.06	3.60	1.20			
	3	6.99	3.63				
Asn ⁷	6	7.70	4.43	2.70			7.23, 6.42 γ -CONH ₂
	6	7.77					7.20, 6.41 γ -CONH ₂
Lys ⁸	[b]	7.42	4.12	1.44	1.64	1.21, 0.96	2.80, 2.66 H ^{ϵ}
							7.22 ϵ -NH
		7.40				1.27, 1.01	2.82, 2.65 H ^{ϵ}
							7.14 ϵ -NH
Leu ⁹	[b]	7.35	4.33	1.61	1.49	0.89, 0.66	7.04, 6.66 α -CONH ₂
		7.36	4.35	1.60	1.45	0.83, 0.63	

Table 4b. Deuteroporphyrin ¹H assignments.

2,18 α,α' -CH ₂	4.90, 4.30	7CH ₃	3.81	13H	9.35
2,18 β,β' -CH ₂	3.30, 3.10	8H	9.35	15H	10.32
3CH ₃	3.77	10H	10.28	17CH ₃	3.73
5H	10.48	12CH ₃	3.75	20H	10.34

[a] Bold values correspond to differentiated resonances for homologous residues belonging to different peptide chains. [b] Not measurable because resonances overlap.

uated from 1D spectra or DQF-COSY when resonances were overlapping. Table 4 reports all the proton chemical shifts and ³J_{NH α CH} coupling constant values. The bottom part of Figure 5b shows the NOESY spectrum with a mixing time of 250 ms.

As for the Δ isomer, the chemical shifts of the peptide residues show a significant upfield shift when compared with typical random coil values.^[23] α -CH and amidic NH proton chemical shift changes are reported on bar charts in Figure 6b. This effect is shown by amidic NH and α -CH as well as by sidechain protons, and is particularly strong for the central His⁵ residue. However, the two peptide chains show slightly different deviations. This may correspond partly to a different orientation of the peptide chains relative to the deuteroporphyrin plane and partly to a different secondary structure of the peptide chains.^[23, 25–26]

The pattern of NOE connectivities strongly supports the existence of a well-organized structure of the peptide chains, even though there is less regularity in comparison with the Δ isomer. A total of 240 short-range and 28 long-range NOE connectivities were measured. Both peptide chains show a very similar pattern of NOEs and their relative intensities are summarized in Figure 12. A continuous stretch of d_{N_iN_{i+1}} NOEs was monitored along the entire peptide sequence, but d _{α _{N_iN_{i+1}}} and d _{β _{N_iN_{i+1}}} connectivities are absent around the His⁵ residues. The C-terminal part, however, displays only a few of the connectivities expected for a helical conformation. Thus an α -helical structure can be inferred for the N-terminal part, while an irregular structure occurs at the C-terminal end. The ³J_{NH α CH} coupling constant values (see Table 4) are also in agreement with this conclusion.

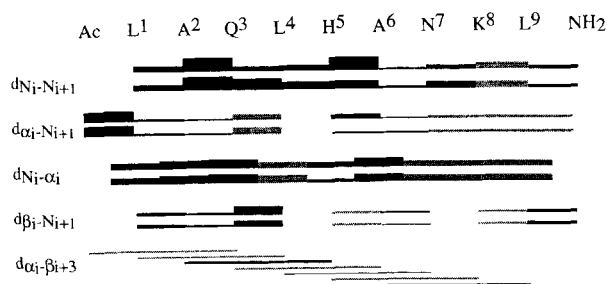


Figure 12. NOE connectivities observed for Co^{III} mimochrome I A isomer. Solid bars indicate unambiguous NOEs. Bar thickness is proportional to NOE intensity. For each row the upper and lower lines refer to the peptide chain linked to the propionyl group in position 18 and 2, respectively.

NOE contacts of the histidine protons with Leu¹ protons were observed for both peptide chains, and they proved essential for the determination of the His⁵ sidechain orientation with respect to the peptide backbone. Co^{III} axial ligation occurs through the unprotonated imidazole N_ε atom of the histidines. As is the case for the Δ isomer, the ε-CH and δ-CH imidazole protons appear in the high-field region of the spectrum because of an extremely large ring-current effect of the deuteroporphyrin. The imidazole protons belonging to the two different histidine residues do not exhibit the same chemical shift. A slight upfield displacement of 0.04 ppm of one of the two histidines is observed. A different positioning of the imidazole rings with respect to the deuteroporphyrin plane may be responsible for this effect.

Furthermore, the δ-CH and ε-CH protons of the histidines have different connectivities with the deuteroporphyrin protons. One histidine exhibits ε-CH↔10H, ε-CH↔8H and δ-CH↔20H dipolar contacts, the other histidine exhibits only ε-CH↔15H and δ-CH↔5H NOEs (Figure 8b). One imidazole ring presumably lies in a plane which is orthogonal to the deuteroporphyrin plane, intersecting it through the 9 and 19 positions of the deuteroporphyrin. The other imidazole ring is located on a plane which is orthogonal to the deuteroporphyrin plane and cuts it through the 15H and 5H protons. This is indicative of an angle of approximately 105° between the imidazole planes. Figure 8b describes the imidazole orientation to the deuteroporphyrin plane, taking into account all the experimental observations. The μ angles are –45° and –60°.

Several NOE contacts between peptide sidechains and deuteroporphyrin protons were measured in the NOESY spectra (mixing time 250 ms). Dipolar contacts are shown in particular by leucine and lysine sidechains. Figure 9b depicts qualitatively the final interpretation.

Figure 10b describes the approximate orientation of the Leu¹, Leu⁴, His⁵, Lys⁸, and Leu⁹ sidechains facing the deuteroporphyrin plane. For the Δ isomer, chain A was identified as the one bound to the propionyl group in position 18, and chain B to the propionyl group in position 2. Furthermore, owing to the right-handedness of the *N*-terminal α-helices, chain A must lie below the plane of the deuteroporphyrin as it is oriented in Figure 9b, and consequently chain B is located above this plane. The complete stereochemistry of the Δ isomer is reported in Figure 11.

Conformational energy calculations: The very large amount of information from CD spectra, interproton NOE effects, and ³*J* coupling constants allowed us to build two approximate models for the Δ and Λ isomers with great confidence. In particular, two regular nonapeptide helices were constructed from standard conformational parameters of an α-helix ($\phi = -63^\circ$, $\psi = -42^\circ$)^[23] for the Δ isomer. The two His⁵ sidechain conformations were both initially set at $\chi^1 = -60^\circ$ and $\chi^2 = 90^\circ$. These helices were placed on opposite sides of the deuteroporphyrin plane, with their axes roughly parallel to it. The relative orientation of the two helices was chosen to be antiparallel, with the N_ε atom of the histidine residues pointing toward the center of the deuteroporphyrin ring at a distance of about 2 Å, and with the imidazole ring planes approximately orthogonal to the deuteroporphyrin plane. The μ angles (Cδ–N_ε–Co–N21) were then set to 45° and 165° by rotation of the entire peptide moieties around the Co–N_ε bond. Subsequently, a more accurate positioning of the helices was achieved by means of the plentiful information from the NOEs between leucine, histidine, and lysine sidechain protons and deuteroporphyrin protons. Finally, simple modeling of the lysine sidechain and propionyl conformation was performed to bring these groups to bonding distance. In order to account simultaneously for all the NOEs and to build a refined molecular structure, molecular dynamics simulations with distance restraints were performed. These calculations were, however, inaccurate because of the lack of an adequate force-field description in the software package for the Co^{III} ion, and therefore all RMD calculations were run without the Co^{III} ion. The coordination force of the Co^{III} ion was instead mimicked with distance restraints between the imidazole atoms and the pyrrole nitrogens. The average backbone molecular conformation along the trajectory of the RMD is reported in Table 5. The refined molecular model is shown in Figure 13a.

The Δ isomer is characterized by two peptide chains with very similar conformation. The φ, ψ angles from Leu¹ to Lys⁸ are

Table 5. Torsion angles (°) of the average conformation derived from RMD for Co^{III} mimochrome I Δ and Λ isomers: (A) is the peptide chain linked to the propionyl group at position 18 of the deuteroporphyrin ring; (B) is the peptide chain linked to the propionyl group at position 2 of the deuteroporphyrin ring.

	Δ A			Δ B			Λ B			Λ A		
	φ	ψ	χ ¹	φ	ψ	χ ¹	φ	ψ	χ ¹	φ	ψ	χ ¹
Leu ¹	–71	–21	–66	–69	–27	–65	–75	–38	–53	–78	–45	–67
Ala ²	–67	–47		–67	–49		–48	–37		–48	–46	
Gln ³	–72	–31	–163	–68	–36	–164	–54	–45	–156	–57	–47	–168
Leu ⁴	–51	–47	–173	–52	–47	–177	–68	–40	–71	–57	–43	–61
His ⁵	–93	–24	–67	–82	–32	–64	–77	–19	–59	–75	–38	–66
Ala ⁶	–62	–31		–67	–26		–63	–41		–46	–55	
Asn ⁷	–62	–30	–75	–59	–33	–78	–62	–38	–168	–65	–18	–170
Lys ⁸	–98	–59	–47	–90	–40	–47	73	–89	–177	76	–79	–171
Leu ⁹	–88	–79	–69	–110	66	–61	–130	49	–72	–128	69	–149

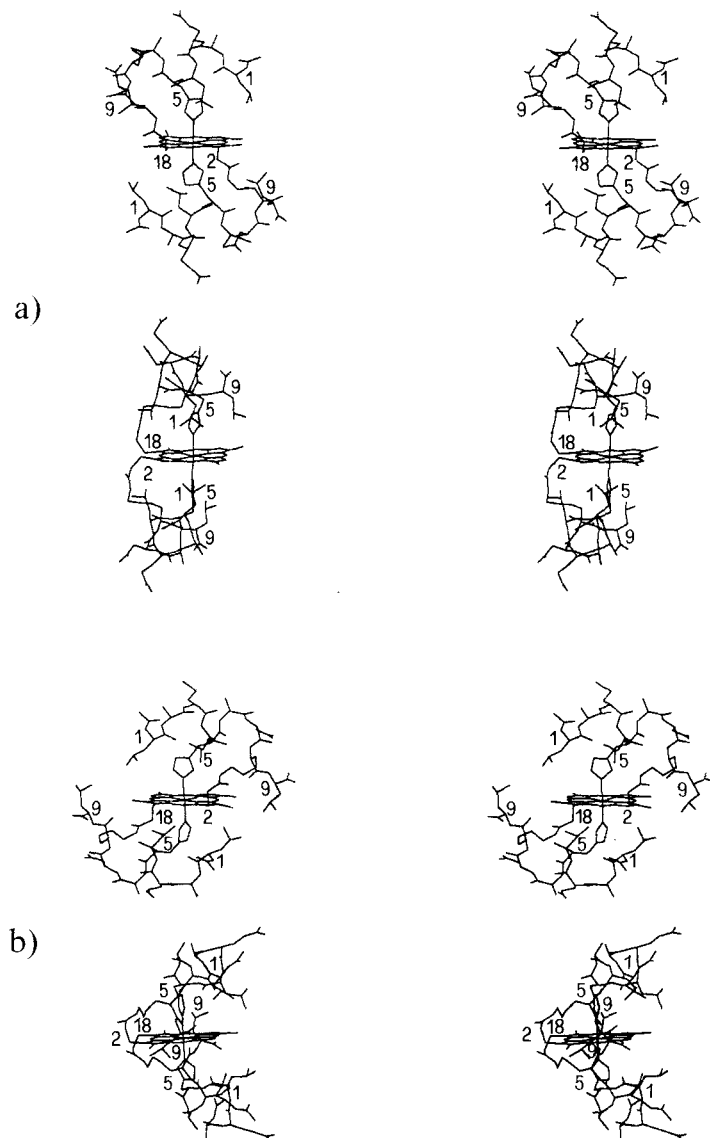


Figure 13. Front and side stereo views of the average molecular structure obtained from RMD simulations for Co^{III} mimochrome I Δ isomer (a) and Λ isomer (b).

very close to those expected for a right-handed α -helical conformation,^[23] although a small distortion toward a 3_{10} -helical conformation^[27] is observed around the Ala⁶–Asn⁷ segment. All peptide bonds are *trans* and all sidechain conformations are staggered. An almost regular $C_iO_i \rightarrow HN_{i+4}$ pattern of intramolecular hydrogen bonds is observed for both peptide chains (see Table 6). Weaker interactions were found: a) at the *N*-terminal acetyl protecting group, presumably because of the lack of a *N*-capping motif; b) at Gln³–C'O \rightarrow Asn⁷–NH, because of a hydrogen bond involving the Asn⁷ sidechain; c) at Leu⁴–C'O \rightarrow Lys⁸–NH, because of the constrained conformational space around the Lys⁸ residue, which must be adapted to achieve the His⁵–Co axial coordination. Furthermore, the His⁵–C'O group is hydrogen-bonded to both the Lys⁸ and Leu⁹ NHs, giving rise to a type III β -turn inserted in a type I α_{RS} -turn.^[28] Both His⁵ δ -NH groups are hydrogen-bonded with the Leu¹ C'O groups. The molecule contains a pseudo- C_2 axis relating the two peptide chains. It passes through the posi-

Table 6. Intrachain N–O distances (Å) of the average structure derived from RMD for Co^{III} mimochrome I Δ and Λ isomers: (A) peptide chain linked to the propionyl group at position 18 of the deuteroporphyrin ring; (B) peptide chain linked to the propionyl group at position 2 of the deuteroporphyrin ring. O₀ refers to the acetyl CO group.

Donor	Acceptor	Δ A	Δ B	Λ B	Λ A
N ₃	O ₀	4.4	3.8	3.7	4.4
N ₄	O ₀	4.2	3.8	4.4	4.6
N ₅	O ₁	3.3	3.4	3.3	3.5
N ₅ ^b	O ₁	2.9	2.9	3.1	2.8
N ₆	O ₂	2.9	2.9	2.9	3.0
N ₇	O ₃	3.9	3.5	4.0	3.4
N ₇ ^c	O ₃	3.0	2.9		
N ₈	O ₄	4.4	4.5	3.2	3.6
N ₈ ^e	O ₄	4.0	4.0		
N ₈	O ₅	3.1	3.1	3.3	3.3
N ₉	O ₅	3.1	3.3		

tions 9 and 19 of the deuteroporphyrin ring. When superimposing the C α atoms of one chain onto the C α atoms of the other, a root mean square displacement of 0.45 Å was measured for these atoms.

The approximate model for the Λ isomer was built in a manner similar to that used for the Δ isomer, except for the μ angles (C δ –N ϵ –Co–N21), which were set to -60° and -45° . Subsequently, a more accurate positioning of the helices was achieved from all the information on the NOEs between Leu¹, Leu⁴, and His⁵ sidechain protons and the deuteroporphyrin protons. The helix axes were then found to form an angle of about 105° . Finally, Lys⁸ and Leu⁹ conformations were substantially modified from those of a regular helix both to orient the Leu⁹ sidechain protons properly with respect to the deuteroporphyrin protons and to bring the Lys⁸ sidechain and the propionyl groups to bonding distance. This modeling brought a reversal of the helix handedness at the *C*-terminal end. As with the Δ isomer, the Co^{III} ion was not included in the calculations and the coordination force of the Co^{III} ion was mimicked with distance restraints between the imidazole atoms and pyrrole nitrogens. This model was subjected to RMD simulation in vacuo. The average backbone molecular conformation along the trajectory of the RMD is reported in Table 5. The refined molecular model is shown in Figure 13b.

The Λ isomer is characterized by two peptide chains with very similar conformation. The ϕ , ψ angles are very close to those expected for a right-handed α -helical conformation,^[23] except for the Lys⁸ and Leu⁹ *C*-terminal residues. Again, all peptide bonds are *trans* and all sidechain conformations are staggered, and an almost regular $C_iO_i \rightarrow HN_{i+4}$ pattern of intramolecular hydrogen bonds is observed for both peptide chains (see Table 6) except for the presence at the *C*-terminal end of a His⁵–C'O \leftarrow Lys⁸–NH and the lack of a His⁵–C'O \leftarrow Leu⁹–NH hydrogen bond. As was the case for the Δ isomer, weaker interactions were found at the *N*-terminal acetyl protecting group and at Gln³–C'O \rightarrow Asn⁷–NH. Both His⁵ δ -NH groups are hydrogen-bonded with the Leu¹ C'O groups. The molecule contains a pseudo- C_2 axis relating the two peptide chains, which passes through positions 10 and 20 of the deuteroporphyrin ring. When superimposing the C α atoms of one chain onto the C α atoms of the other, a root mean square displacement of 0.50 Å was measured for these atoms.

Discussion

The incorporation of cobalt in the free base mimochrome I yields two different species in about equal amounts with the expected molecular mass. The identification of these species was rather difficult for a number of reasons; for instance, the metal ion may present: a) in different oxidation states; b) with different axial ligation; c) with different stereochemistry. The peptidic part may have undergone: a) racemization during the synthesis; b) chemical rearrangement of the amino acid side chain, such as asparagine \rightleftharpoons iso-asparagine interconversion; c) peptide-bond *cis* \leftrightarrow *trans* isomerism; d) conformational transition. The acid-catalyzed interconversion between the two species allowed us to exclude the possibility of a racemic mixture. This preliminary experiment suggested possible involvement of the metal-ion coordination in determining the differences between these two species. It was reasonable to hypothesize that at very low pH the histidine residues might become protonated, favoring the disruption of the axial coordination. Furthermore, the slow kinetics of interconversion between the Δ and Λ species could also be indicative of a complex molecular process. The stability of both species to air oxidation and the UV/visible spectra allowed us to ascertain the absence of multiple oxidation states of the cobalt ion. The Co^{II} complexes are in fact characterized by a λ_{max} Soret band at ≈ 390 nm, and they show a typical two-banded spectrum in the β and α region, in which the longer wavelength band has a higher intensity ($\beta = 518$ nm, $\epsilon = 10300 \text{ M}^{-1} \text{ cm}^{-1}$; $\alpha = 551$ nm, $\epsilon = 21700 \text{ M}^{-1} \text{ cm}^{-1}$).^[12] In contrast, octahedral Co^{III} porphyrins are identified by β and α bands of approximately equal intensity ($\beta = 529$ nm, $\epsilon = 10900 \text{ M}^{-1} \text{ cm}^{-1}$; $\alpha = 561$ nm, $\epsilon = 11500 \text{ M}^{-1} \text{ cm}^{-1}$) and a red shift of the Soret band to ≈ 416 nm.^[12] The spectral data are all in agreement with an octahedral Co^{III} porphyrin derivative for both species. The Soret bands of both the Δ and Λ isomers are very sharp; the linewidth is about 15 nm. The differences in the extinction coefficients at the Soret maximum can tentatively be attributed to different transition moments in the two isomers, which may derive from both the different deuteroporphyrin π orbitals overlapping with imidazole π orbitals and/or metal d orbitals.

CD measurements in both the far UV and the Soret region partly clarified the structural differences of these two species. The effect of the helix-inducing solvent TFE on the CD spectra of the Δ and Λ species was analyzed. The Δ isomer is characterized by a helical conformation even at 0% TFE, whereas Λ is more randomly coiled. This is clearly indicated by the position and the more intense ellipticity of the maximum at the shorter wavelength found in the Δ isomer. On addition of TFE, both isomers reached the maximum 222 nm ellipticity at 50% TFE, but the values are -9281 and $-6040 \text{ M}^{-1} \text{ cm}^{-1}$ for Δ and Λ isomers, respectively. The other important feature derived from this titration is the presence in the Δ isomer of an isodichroic point at 199.8 nm. This is consistent with the expected C_2 symmetry relating both peptide helical segments. In contrast, the Λ isomer shows independent behavior (coil \leftrightarrow helix transition) of the two helices upon TFE addition. CD measurements in the far UV revealed that the Δ and Λ isomers are characterized by different conformations of the peptidic part, but they may both contain a slight distortion of the α -helical conformation toward

a 3_{10} -helical structure, since $[\theta]_{\text{ratio}}$ is < 1 . However, this low value of $[\theta]_{\text{ratio}}$ may also be interpreted in terms of the interactions between the heme transitions and those of the peptide backbone amide dipoles.^[10e, 29]

More interesting for an understanding of the differences between the Δ and Λ isomers was the study of the CD effect in the Soret region. The Δ and Λ isomers display single band effects of opposite sign and of different intensities. Theoretical calculations indicated that the direction of the polarization of the Soret components B_x and B_y in the heme plane could be affected by the surrounding environment of the heme, thus resulting in a variety of Cotton effects of different shape and complexity.^[30] Porphyrin dianions and their metal-ion derivatives possess high symmetry elements and are expected to be devoid of optical activity. The presence of additional substituents on the porphyrin plane, as in mimochrome I,^[1a] would only partly lower the symmetry of the chromophore. The free base mimochrome I, or Fe^{III} mimochrome I at pH = 2, in which the peptide chains are presumably away from the deuteroporphyrin plane, lacks any optical activity in the Soret region. However, when the peptide chains fold to allow bis(histidine) axial coordination for both the Δ and Λ Co^{III} mimochrome I isomers, and when these chains approach the deuteroporphyrin plane at van der Waals contact distances, the result is optical activity in the Soret region. Again, this can be considered as further evidence that differences between the two isomers are related to different coordination geometries and interactions of the peptide chains with the Co^{III} deuteroporphyrin.

Finally, a definitive answer on the structural differences between the Δ and Λ isomer was derived from ^1H NMR analysis. First of all, we ascertained the structural integrity of both isomers and the absence of any *cis* \leftrightarrow *trans* peptide bond interconversion. The peptide chains of the Δ isomer adopt an almost regular α -helical conformation containing 2.5 turns. A squeezed helical winding is observed at the C-terminal end. This partial distortion toward a 3_{10} -helical arrangement involves the His⁵–Lys⁸ segment in order to accommodate the imidazole rings and the lysine sidechain; this is in good agreement with the CD data in the far UV region, where $[\theta]_{\text{ratio}}$ is about 0.5. The helices are in van der Waals contact through their sidechains with two different faces of the deuteroporphyrin ring. These observations are in agreement with the chemical shifts, which deviate significantly from random coil values.^[23] α -CH chemical shift deviations exceed 0.4 ppm upfield, at least for the first six residues (see Figure 6a). An upfield shift of 0.4 ppm represents the higher expected shift for α -CH protons in a helical arrangement.^[23, 25–26] The larger upfield deviations are therefore consistent with the presence of ring-current effects. Comparison of the experimental ring-current shifts with those calculated from the models will provide an independent check and/or further insight into the hypothetical structures, since the three-dimensional model of Co^{III} mimochrome I Δ isomer was obtained without recourse to ring-current effects.

The peptide helices of the Λ isomer are about antiparallel and they are related by a pseudo- C_2 symmetry axis. The lack of a true C_2 axis derives from the asymmetry of the deuteroporphyrin ring; this also results in a slightly different position of the peptide chains with respect to the deuteroporphyrin plane. In particular, Leu¹, Leu⁴, and Leu⁹ of each peptide chain face

different atoms in the deuteroporphyrin ring. Bisaxial coordination through the $N\epsilon$ atoms of the central His⁵ residues was observed. Both His⁵ δ -NH groups are hydrogen-bonded with the Leu¹ C'O groups. This sidechain \rightarrow backbone hydrogen-bonding is a common feature of several hemoproteins,^[31] and it was proposed as an important structural feature in the electronic properties of the metal ion. The orientation of both imidazole rings was accurately determined on the basis of the NOEs between the deuteroporphyrin protons and the imidazole rings. The μ torsion angles, which indicate the relative orientation of the two imidazole rings with respect to the Co–N21 direction, are different; they are both positive. The μ angle, as defined in this paper, is different from the ϕ angle previously reported.^[32] In our opinion the definition of the μ angle as the torsion angle $C\delta$ -N ϵ -M-N21 (M is the metal ion) is more accurate, because it also contains information about the sign of the angle and is particularly useful for asymmetric ligands. The solution structure derived from the NMR analysis also enabled us to ascertain the configuration around the Co^{III} ion. It is well known that for several reasons the chelating agents can be schematized and their actual conformation ignored. Figure 11 b depicts this approximation, in which the peptide chains have been replaced by two segments connecting the $N\epsilon$ atoms and positions 2 and 18 of the deuteroporphyrin ring. In this schematic presentation the molecule contains a C_2 axis as unique element of symmetry. Therefore, the molecule must be chiral and the two possible forms are enantiomorphs. The Δ isomer is defined as that obtained when, viewed along the $N\epsilon$ -M direction, the closer chain must be rotated clockwise to overlap the other chain. In fact, because of the substituents on the porphyrin ring and the chirality of the peptide chain, the Δ and Λ isomers of Co^{III} mimochrome I are diastereomers.

The peptide structure of Co^{III} mimochrome I Δ isomer is such that leucine and lysine sidechains create a partially open hydrophobic cage around the imidazole ring. This local nonpolar environment may play an important role in determining the electronic properties of the metal ion inserted in the deuteroporphyrin ring.^[33] Position 10 of the deuteroporphyrin ring is exposed to the solvent, while all the other *meso* positions are covered by the polypeptide chains. This particular orientation of the sidechains with respect to the deuteroporphyrin plane may have an important effect in protecting the deuteroporphyrin ring from degradation during catalytic cycles, when a catalytically active metal is contained in the deuteroporphyrin ring, and when this metal does not disrupt the three-dimensional structure of the peptide chains. This protective effect is in fact achieved by the polypeptide matrix in hemoproteins. This may imply that *meso*-unsubstituted porphyrins, when embedded in a well-defined peptide environment, may function efficiently as catalysts. In addition, alanines, glutamines, and asparagines point outward from the molecular core, and may provide sites where amino-acid substitution (with differently charged residues) would alter the electric field around the metal center and therefore modulate the electronic, catalytic, and binding properties of the metal.^[3]

The peptide chains of the Λ isomer adopt a less regular conformation. Only two complete α -helical turns are present. The His⁵-Lys⁸ segment is partially distorted toward a 3_{10} -helical arrangement to better accommodate the imidazole rings and the

lysine sidechain. This is in good agreement with the CD data in the far UV region, where $[0]_{ratio}$ is about 0.4. The peptide sidechains are in van der Waals contact with two different faces of the deuteroporphyrin. The peptide helices are related by a pseudo- C_2 symmetry axis. Leu¹, Leu⁴, and Leu⁹ of one peptide chain face different atoms of the deuteroporphyrin ring when compared with the same residues of the other chain. Bisaxial coordination through the $N\epsilon$ atoms of the central His⁵ residues was determined. Both imidazole rings were positioned precisely according to the NOEs between the deuteroporphyrin protons and those of the imidazole rings. As was the case for the Δ isomer, the μ angles relative to the imidazole rings of the two peptide chains exhibit different values, but unlike those in the Δ isomer, they are both negative. The solution structure derived from the NMR analysis and RMD calculations in vacuo also enabled us to ascertain the configuration around the Co^{III} ion. Figure 11 b schematically depicts the configuration around the metal. The helical structure of the peptide chains in the Λ isomer is such that Leu¹, Leu⁴, His⁵, and Lys⁸ sidechains are facing the deuteroporphyrin plane, while the Leu⁹ sidechain faces one side of the deuteroporphyrin plane. Leucines and lysine sidechains create a partially open hydrophobic cage around the imidazole ring. Position 20 of the deuteroporphyrin ring is exposed to the solvent. Alanines, glutamines and asparagines are instead pointing outward from the molecular core.

Conclusions

The present paper reports the synthesis and purification of two stable diastereomeric forms (Δ and Λ) of Co^{III} mimochrome I. The solution three-dimensional structure of Co^{III} mimochrome I Δ and Λ isomers is the first example, to the best of our knowledge, of a well-characterized peptide-based hemoprotein model; the structure of the Δ isomer confirms the design hypothesis. The structures of Co^{III} mimochrome I Δ and Λ isomers will allow a quantitative interpretation of: a) the ring-current effect on the proton chemical shifts; b) the differences in the absorption coefficients in the UV/visible transitions; c) the origin of the Soret-region induced Cotton effect. Furthermore, these structures can serve as template structures for the design of novel molecules with predetermined electronic and binding properties.

Experimental Procedure

Mimochrome I: The free base deuteroporphyrin-bis(nonapeptide) adduct mimochrome I (3,7,12,17-tetramethylporphyrin-2,18-di- $N_{\delta\epsilon}$ -(Ac-Leu¹-Ala²-Gln³-Leu⁴-His⁵-Ala⁶-Asn⁷-Lys⁸-Leu⁹-NH₂)propionamide was obtained as described in the previous paper.^[1a]

Cobalt insertion: The cobalt was inserted into mimochrome I according to the literature procedure.^[11] Cobalt(II) acetate (0.015 g, 5.8×10^{-5} mol) was added to a solution of pure mimochrome I (0.030 g, 1.17×10^{-5} mol) in acetic acid/TFE 6:4 (v/v, 60 mL). The reaction mixture was kept under reflux for 2 h at 50 °C. The reaction was monitored by analytical HPLC (see below). The HPLC analysis of the reaction mixture revealed the presence of two major peaks ($R_t = 14.92$ and 15.31 min, respectively) in nearly equal amounts (Figure 2). The retention time of the starting material mimochrome I is 16.8 min under the same experimental conditions. Air was bubbled through the reaction mixture in order to investigate whether the two peaks resulted

from incomplete $\text{Co}^{\text{II}} \rightarrow \text{Co}^{\text{III}}$ oxidation. The solvent was then removed under vacuum, and the two peaks, named Δ ($R_t = 14.92$ min) and Λ ($R_t = 15.31$ min), were finally separated by preparative HPLC. 0.0058 g of pure Δ and 0.0060 g of pure Λ were obtained as TFA salts. Analytical HPLC confirmed the purity of both products. FAB mass spectrometry of both Δ and Λ species gave molecular ion peaks [M^+] of $M_r = 2625$, corresponding to that expected for Co^{III} mimochrome I.

HPLC procedure: Analytical reverse-phase high-performance liquid chromatography was performed on a Varian 3000 LC Star System, equipped with a 9065 Polychrom and a 9095 Autosampler. A Vydac C18 column (4.6×150 mm; $5 \mu\text{m}$), eluted with a $\text{H}_2\text{O}/0.1\%$ trifluoroacetic acid (TFA) (A) and $\text{CH}_3\text{CN}/0.1\%$ TFA (B) linear gradient from 20 to 80% B over 25 min, at 1 mL min^{-1} flow rate, was used in all the analyses. A Water Delta Prep 3000 HPLC, equipped with an UV Lambda-Max Mod 481 detector, was used for product purification. A linear gradient from 20 to 80% of B over 40 min at flow rate of 114 mL min^{-1} on a Vydac C18 column (50×250 mm; $10 \mu\text{m}$) was employed in all purifications. $3.0 \times 10^{-4} \text{ M}$ solutions were prepared by dissolving the corresponding complex (0.4 mg, $1.5 \times 10^{-5} \text{ mol}$) in TFE (0.5 mL). The solutions were kept at room temperature and subsequent HPLC injection (20 μL volume) for both species was performed at different intervals after dissolution ($t = 0, 4, 18, 48$ h). Likewise, $3.0 \times 10^{-4} \text{ M}$ solutions in TFE/acetic acid 1:1 (acid concentration 8.7 M) were prepared for both Δ and Λ species, in order to evaluate their relative stability in acid conditions. Subsequent injections (20 μL) were performed at different times ($t = 0, 4, 18, 48, \text{ and } 96$ h). The amount of the two species was calculated by measuring the HPLC peak areas.

Sample preparation for spectroscopic characterization: Co^{III} mimochrome I stock solutions ($2.0 \times 10^{-4} \text{ M}$) in TFE were prepared for both Δ and Λ species. These solutions were then diluted to about $1.0 \times 10^{-5} \text{ M}$ with different amounts of aqueous phosphate (pH 7.0 and 1.0) and TFE. The TFE/aqueous phosphate ratio was varied from 10% to 50% (v/v); the final phosphate concentration was $3.0 \times 10^{-4} \text{ M}$. A $1.0 \times 10^{-5} \text{ M}$ solution in $3.0 \times 10^{-4} \text{ M}$ phosphate (pH 7.0) was also prepared. Final concentrations were determined spectrophotometrically at the Soret maximum wavelength with extinction coefficients calculated from Lambert and Beer's law.

UV/Visible spectroscopy: UV/Vis spectra were recorded on a Perkin Elmer Lambda 7 UV Spectrophotometer with 1 cm path length cells. Wavelength scans were performed at 25°C from 200 to 700 nm, with a 60 nm min^{-1} scan speed. Sample concentrations in the range $1.0 \times 10^{-6} - 1.0 \times 10^{-5} \text{ M}$ were used for the determination of the extinction coefficient at the Soret maximum wavelength.

Circular dichroism measurements: CD measurements were obtained at 25°C by means of a Jasco J-700 dichrograph calibrated with an aqueous solution of recrystallized D(+)-10-camphorsulfonic acid at 290 nm.^[34] Data were collected at 0.2 nm intervals, with a 5 nm min^{-1} scan speed, a 1 nm bandwidth, and a 16 s response, from 260 to 185 nm in the far UV region and from 450 to 260 nm in the Soret region; cuvette path lengths of 1 cm were used for both spectral regions. CD spectra were corrected by subtraction of the background solvent spectrum obtained under identical experimental conditions and were smoothed for clarity of display. The experiments were carried out on the same solutions used for the UV/vis measurements. CD intensities in the far UV region are expressed as mean residue ellipticities ($^\circ\text{cm}^2\text{dmol}^{-1}$), calculated by dividing the total molar ellipticities by the number of amino acids in the molecule; intensities in the Soret region are reported as total molar ellipticities.

^1H NMR spectroscopy: ^1H NMR 1D and 2D spectra were acquired on a Varian Unity 400 spectrometer operating at 400 MHz and equipped with a Spac station SUN 330. Co^{III} mimochrome I was used as a $1.0 \times 10^{-3} \text{ M}$ solution in $\text{H}_2\text{O}/\text{CF}_3\text{CD}_2\text{OD}$ 30:70 (v/v) (pH = 4.5). Conventional pulse sequences were used for TOCSY, NOESY, ROESY, and DQF-COSY. All 2D spectra were recorded in pure absorption mode with the States-Haberkmorn method and were usually acquired with a spectral width of 5.4 kHz, 256 t_1 points, 4 K data points in t_2 , and 32 transients for each t_1 increment. Prior to 2D Fourier transformation, the data were usually multiplied by shifted sine bells in both t_2 and t_1 and zero-filled to 4 K or 8 K \times 1 K data points. The water resonance was generally suppressed by continuous low-power irradiation at all times except during t_2 . For TOCSY experiments a typical value of

70 ms was used as mixing time. NOESY spectra were recorded with mixing time values ranging from 120 to 400 ms. Semiquantitative information on interproton distances for the structure determination was obtained by analyzing the 250 ms NOESY spectra that did not exhibit any spin diffusion effects.^[35] Crosspeak volumes were integrated on both sides of the diagonal and averaged. These volumes were converted into distance restraints by means of the crosspeak volume between the β - and β' - CH_2 protons of Gln³ (1.75 \AA). DQF-COSY spectra were collected over 6500 complex points with 112 transients for each of the 512 t_1 increments. The spectral width was reduced to 3.8 kHz in t_1 and t_2 dimensions. The data matrix was zero-filled to yield a final digital resolution of 0.5 Hz and 3.7 Hz in the t_1 and t_2 dimensions, respectively. All reported proton chemical shifts are relative to the sodium salt of [D₄]3-(trimethylsilyl)propionic-2,2,3,3 acid (TSP) at 298 K.

Conformational energy calculations: Restrained Molecular Dynamic simulations (RMD) were performed on a Personal Iris 4D35 GT Turbo Silicon Graphics workstation with the DISCOVER program v 2.9, Consistent Valence Force Field (CVFF),^[36–38] and a time step of 0.5 fs. All simulations were carried out in vacuo at 300 K and the computational conditions were chosen to avoid boundary condition effects.^[39] The equations of motion were solved with the leapfrog algorithm.^[40] The starting models were hand-built from standard parameters for amino acid residues supplied with the INSIGHT software package^[41] and structural parameters from NMR measurements (e.g., interproton distances from NOE values and $^3J_{\text{NH}\alpha\text{CH}}$ coupling constants). The distance restraints in the RMD calculations were classified according to the relative intensity of the NOEs into three classes: 1.8–2.6 (strong), 2.5–3.3 (medium), and 3.2–4.1 Å (weak). RMDs were run on the free mimochrome I base because of the lack of an implemented force field for the Co^{III} ion in the Discover package. The coordination force of the Co^{III} ion was approximately simulated as follows: a) the deuteroporphyrin ring was forced to be flat; b) distance restraints were introduced between the imidazole atoms and pyrrole nitrogen by the use of a force constant as strong as that used for the interproton distances accounting for the NOE effects. The distances were allowed to deviate in a range of $\pm 0.2 \text{ \AA}$. Reference distances were selected from the X-ray structure of other Co^{III} porphyrin complexes.^[42] The imidazole rings were forced to lie with their planes orthogonal to the deuteroporphyrin plane. The orientation of the imidazole ring relative to the deuteroporphyrin plane and to the *meso* positions was deduced from the NOE contacts with the deuteroporphyrin protons. All simulations were carried out for 50 ps in the equilibration phase, and for 250 ps without velocity rescaling since the temperature remained constant at around 300 K.

Acknowledgments: We are grateful to Dr. D. Mansuy and P. Battioni (Paris, France) for helpful discussions. This work is part of the Ph.D. thesis of Dr. Flavia Nastri and was supported by the Italian C. N. R., grant no. 113.156-14 (1995).

Received: August 5, 1996 [F 431]

- [1] a) F. Nastri, A. Lombardi, G. Morelli, O. Maglio, G. D'Auria, C. Pedone, V. Pavone, *Chem. Eur. J.* **1997**, *3*, 340–349; b) F. Nastri, A. Lombardi, O. Maglio, G. Morelli, G. D'Auria, V. Pavone, C. Pedone, *Fourth Naples Workshop on Bioactive Peptides*, Capri (Italy), **1994**, 86; c) A. Lombardi, F. Nastri, O. Maglio, G. Morelli, V. Pavone, C. Pedone, P. Battioni, D. Mansuy, G. Chottard, *Metal Ions in Biological Systems, Eurobic II*, Florence (Italy) **1994**, 218; d) F. Nastri, A. Lombardi, O. Maglio, G. Morelli, G. D'Auria, C. Pedone, V. Pavone, *Syntheses and Methodologies in Inorganic Chemistry* (Eds.: S. Daolio, E. Tondello, P. A. Vigato), Photograf, Padova (Italy), **1995**, 5, 242–245.
- [2] *The Porphyrins*, Vol. 7 (Ed.: D. Dolphin), Academic Press, New York, **1979**.
- [3] D. S. Wuttke, H. B. Gray, *Curr. Opin. Struct. Biol.* **1993**, *3*, 555–563.
- [4] R. A. Sheldon, *Metalloporphyrins in Catalytic Oxidations*, Marcel Dekker, New York, **1994**.
- [5] a) B. Meunier, *Chem. Rev.* **1992**, *92*, 1411–1456; b) D. Mansuy, P. Battioni, J. P. Battioni, *Eur. J. Biochem.* **1989**, *184*, 267–285; c) D. Mansuy, *Pure Appl. Chem.* **1990**, *62*, 741–746; d) J. P. Collman, X. Zhang, V. J. Lee, E. S. Uffelman, J. I. Brauman, *Science* **1993**, *261*, 1404–1411.
- [6] a) J. W. Buchler, B. Scharbert, *J. Am. Chem. Soc.* **1988**, *110*, 4272–4276; b) J. L. Sessler, B. Wang, A. Harriman, *ibid.* **1993**, *115*, 10418–10419; c) H. Grennberg, S. Faizon, J. E. Bäckvall, *Angew. Chem. Int. Ed. Engl.* **1993**, *32*, 263–264; d) L. Sun, J. von Gersdorff, D. Niethammer, P. Tian, H. Kurreck, *ibid.* **1994**, *33*, 2318–2320; e) J. T. Groves, T. E. Nemo, R. S. Myers, *J. Am. Chem. Soc.* **1979**, *101*, 1032–1028; f) M. Momentau, B. Loock, J. Mispelner, E. Bisagni, *Nouv. J. Chim.* **1979**, *3*, 77–84.

- [7] a) J. P. Collmann, R. R. Gagne, C. A. Reed, T. R. Halbert, G. Lang, W. T. Robinson, *J. Am. Chem. Soc.* **1975**, *97*, 1427–1439; b) T. G. Traylor, C. K. Chang, J. Geibel, A. Berzini, T. Mincey, J. Cannon, *ibid.* **1979**, *101*, 6716–6731; c) K. S. Suslick, M. M. Fox, *ibid.* **1983**, *105*, 3507–3510.
- [8] a) P. A. Adams, M. P. Byfield, R. C. de L. Milton, J. M. Pratt, *J. Inorg. Biochem.* **1988**, *34*, 167–175; b) T. Mashino, S. Nakamura, M. Hirobe, *Tetrahedron Lett.* **1990**, *31*, 3163–3166.
- [9] a) C. T. Choma, J. D. Lear, M. J. Nelson, P. L. Dutton, D. E. Robertson, W. F. DeGrado, *J. Am. Chem. Soc.* **1994**, *116*, 856–865; b) D. E. Robertson, R. S. Farid, C. C. Moser, J. L. Urbauer, S. E. Mulholland, R. Pidikiti, J. D. Lear, A. J. Wand, W. F. DeGrado, P. L. Dutton, *Nature* **1994**, *368*, 425–432; c) T. Sasaki, E. T. Kaiser, *J. Am. Chem. Soc.* **1989**, *111*, 380–381; d) T. Sasaki, E. T. Kaiser, *Biopolymers* **1990**, *29*, 79–88.
- [10] a) L. Casella, M. Gullotti, L. De Gioia, E. Monzani, F. Chillemi, *J. Chem. Soc. Dalton Trans.* **1991**, 2945–2953; b) L. Casella, M. Gullotti, L. De Gioia, R. Bartesaghi, F. Chillemi, *ibid.* **1993**, 2233–2239; c) B. Pispisa, M. Venanzi, M. D'Alagni, *Biopolymers* **1994**, *34*, 435–442; d) Y. Ohkatsu, T. Watanabe, T. Goto, M. Wakita, *Bull. Chem. Soc. Jpn.* **1994**, *67*, 742–747; e) D. R. Benson, B. R. Hart, X. Zhu, M. B. Doughty, *J. Am. Chem. Soc.* **1995**, *117*, 8502–8510.
- [11] J. W. Buchler, in *The Porphyrins, Vol. 1* (Ed.: D. Dolphin), Academic Press, New York, **1979**, pp. 389–483.
- [12] A. W. Johnson, I. T. Kay, *J. Chem. Soc.* **1960**, 2979–2983.
- [13] a) M. Momenteau, D. Lexa, *Biochem. Biophys. Res. Commun.* **1974**, *58*, 940–944; b) R. Bonnet, M. J. Dimsdale, *J. Chem. Soc.* **1972**, 2540–2548.
- [14] a) N. Greenfield, G. D. Fasman, *Biochemistry* **1969**, *8*, 4108–4116; b) M. Mutter, K. H. Altman, A. Florsheimer, J. Herbert, *Helv. Chim. Acta* **1986**, *69*, 786–792; c) M. C. Manning, R. W. Woody, *Biopolymers* **1991**, *31*, 569–586; d) S. Vuilleumier, M. Mutter, *ibid.* **1993**, *33*, 389–400.
- [15] E. K. S. Yijayakumar, T. S. Sudha, P. Balaram, *Biopolymers* **1984**, *23*, 877–886.
- [16] a) A. Jasanoff, A. R. Fersht, *Biochemistry* **1994**, *33*, 2129–2135; b) R. Bonnett, M. J. Dimsdale, *J. Chem. Soc. Perkin. I* **1972**, 2540–2548.
- [17] A. Bax, D. G. Davis, *J. Magn. Reson.* **1985**, *65*, 355–360.
- [18] J. Jeener, B. H. Meier, P. Backman, R. R. Ernst, *J. Chem. Phys.* **1979**, *71*, 4546–4553.
- [19] A. A. Bothner-By, R. L. Stephens, C. D. Warren, R. W. Jeanloz, *J. Am. Chem. Soc.* **1984**, *106*, 811–813.
- [20] U. Piantini, O. W. Sorensen, R. R. Ernst, *J. Am. Chem. Soc.* **1982**, *104*, 6800–6801.
- [21] R. M. Keller, K. Wuthrich, *Biochem. Biophys. Res. Commun.* **1978**, *83* (B), 1132–1139.
- [22] K. Wuthrich, *NMR of Proteins and Nucleic Acids*, Wiley, New York, **1986**.
- [23] D. S. Wishart, B. D. Sikes, F. M. Richards, *J. Mol. Biol.* **1991**, *222*, 311–333.
- [24] R. D. Guiles, J. Altman, I. D. Kuntz, L. Waskell, *Biochemistry* **1990**, *29*, 1276–1289.
- [25] A. Pastore, V. Saudek, *J. Magn. Reson.* **1990**, *90*, 165–176.
- [26] K. Osapay, D. A. Case, *J. Biomol. NMR* **1994**, *4*, 215–230.
- [27] E. Benedetti, B. Di Blasio, V. Pavone, C. Pedone, C. Toniolo, M. Crisma, *Biopolymers* **1992**, *32*, 453–456.
- [28] V. Pavone, G. Gaeta, A. Lombardi, F. Nistri, O. Maglio, C. Isernia, M. Saviano, *Biopolymers* **1996**, *38*, 705–721.
- [29] M. Nakano, H. Iwamaru, T. Tobita, J. T. Yang, *Biopolymers* **1982**, *21*, 805–815.
- [30] M.-C. Hsu, R. W. Woody, *J. Am. Chem. Soc.* **1971**, *93*, 3515–3523.
- [31] J. S. Valentine, R. P. Sheridan, C. A. Leland, P. C. Kahn, *Proc. Natl. Acad. Sci. USA* **1979**, *76*, 1009–1013.
- [32] W. R. Scheidt, D. M. Chipman, *J. Am. Chem. Soc.* **1986**, *108*, 1163–1167.
- [33] R. J. Kassner, *J. Am. Chem. Soc.* **1973**, *95*, 2674–2677.
- [34] W. C. Johnson, Jr., *Methods Biochem. Anal.* **1985**, *31*, 61–163.
- [35] D. Neuhaus, M. Williamson, *The Nuclear Overhauser Effect in Structural Conformation Analysis*, VCH, New York, **1989**, pp. 103–140.
- [36] S. Lifson, A. T. Hagler, P. Dauber, *J. Am. Chem. Soc.* **1979**, *101*, 5111–5121.
- [37] A. T. Hagler, P. Dauber, S. Lifson, *J. Am. Chem. Soc.* **1979**, *101*, 5131–5141.
- [38] A. T. Hagler, S. Lifson, P. Dauber, *J. Am. Chem. Soc.* **1979**, *101*, 5122–5130.
- [39] M. Saviano, M. Aida, G. Corongiu, *Biopolymers* **1992**, *31*, 1017–1024.
- [40] L. Verlet, *Phys. Rev.* **1967**, *159*, 98–103.
- [41] Insight II User Guide, Version 2.1.0, Biosym Technologies, San Diego, **1992**.
- [42] J. W. Lauher, J. A. Ibers, *J. Am. Chem. Soc.* **1974**, *96*, 4447–4452.